

COMMUNICATION

[View Article Online](#)
[View Journal](#) | [View Issue](#)

Metal–organic frameworks as solid magnesium electrolytes†

Cite this: *Energy Environ. Sci.*, 2014, 7, 667

M. L. Aubrey, R. Ameloot, B. M. Wiers and J. R. Long*

Received 19th September 2013
Accepted 10th December 2013

DOI: 10.1039/c3ee43143f

www.rsc.org/ees

A series of solid magnesium electrolytes were synthesized *via* the transmetallation of magnesium phenolates to coordinatively unsaturated metal sites lining the pores of the metal–organic frameworks $\text{Mg}_2(2,5\text{-dioxidobenzene-1,4-dicarboxylate})$ and $\text{Mg}_2(4,4'\text{-dioxidobiphenyl-3,3'-dicarboxylate})$. The resulting materials represent a new class of solid magnesium electrolytes that are both crystalline, and exhibit room-temperature ionic conductivities up to 0.25 mS cm^{-1} . The materials reported herein are one-hundred times more conductive at room temperature than any other solid magnesium electrolyte and represent the only class of materials sufficiently conductive for practical consideration in magnesium batteries.

Metal–organic frameworks, or MOFs, are a class of porous crystalline solids composed of metal ions connected *via* multi-functional organic ligands to form a robust three-dimensional architecture that is permanently porous.¹ The modular nature of these materials allows their framework composition and pore dimensions to be tuned *via* judicious selection of the metal ion and organic ligand.² Further, alteration of the internal surfaces through post-synthetic modification has been widely developed, and presents opportunities for manipulating the properties of a crystalline solid to a degree not possible in purely inorganic solid electrolytes.³

The diffusion of selected guest species, both in solution and in the gas phase, within the pores of MOFs has been studied extensively. Notably, some studies have demonstrated significantly greater diffusivities compared to other microporous materials.⁴ For structures with relatively small pores, confinement effects have further been shown to impose a highly

Broader context

Increasing utilization of sustainable energy sources, such as wind and solar power, together with a rapidly growing electrified transportation fleet, necessitates improvements in energy storage technologies based upon cheap and abundant materials. Magnesium batteries could provide a scalable means of high-density energy storage, but their implementation has been plagued by numerous obstacles, including volatility, corrosion, and the pyrophoricity issues associated with the few available liquid electrolytes. To date, very few reports have considered using a crystalline electrolyte material, though this may open the door new methods of cell assembly and design. A mechanically robust crystalline electrolyte may also allow for a smaller separation between electrodes in the assembled cell. However, no such solid magnesium electrolytes exist with electrochemically relevant ionic conductivities at room temperatures. Here, we report a series of metal–organic frameworks impregnated with magnesium phenolates exhibiting record-breaking room-temperature ionic conductivities, sufficiently high for potential use as a solid electrolytes in a practical magnesium batteries at room temperature. The materials reported represent the first in a new class of solid-state multivalent ion conductors.

disordered structure upon polymer guest species, resulting in ionic diffusivities more similar to those found in a molten state.⁵ However, the transport of charged species within MOFs and their electrochemical applications remains a nascent field.⁶ To date, work on ionically conductive MOFs has been almost exclusively focused on proton transport, which can be mechanistically very different from the transport of metal cations.^{7–9} Nevertheless, a number of Li^+ conducting MOFs have been reported, and these have exhibited conductivities as high as 0.3 mS cm^{-1} at room temperature.^{5,10,11} In contrast to polymer electrolytes, intrinsically porous MOF electrolytes have the distinct advantage that conductivity and mechanical properties are not inversely related. This is because ionic movement relies on through-the-pore diffusion instead of polymer chain mobility.

Considering ions of larger size and greater charge density than Li^+ using solid electrolytes with pores large enough to easily accommodate the guest species may enable fast

Department of Chemistry, University of California, Berkeley and Materials Sciences Division, Lawrence Berkeley National Laboratory, Berkeley, CA 94720, USA. E-mail: jrlong@berkeley.edu

† Electronic supplementary information (ESI) available: detailed synthesis or all materials discussed, description of experimental techniques including Langmuir surface area determination, $^1\text{H-NMR}$, elemental analysis, impedance analysis, variable temperature conductivity measurements, powder diffraction and thermogravimetric analysis. See DOI: 10.1039/c3ee43143f

conduction of such ions, a difficult task in polymer or inorganic electrolytes. This is especially true in the case of Mg^{2+} , because materials that have previously been reported either degrade when ion exchange is attempted, conduct only at very high temperatures (*e.g.*, 600 °C), or conduct only in a hydrated state and never above $1 \mu\text{S cm}^{-1}$ at room temperature.^{12–16} Here, we present the preparation and characterization of a series of solid Mg^{2+} electrolytes in which a MOF host framework can mediate remarkably facile ion transport, achieving rates unprecedented in other classes of crystalline materials.

We hypothesized that MOFs with a high density of open metal sites capable of coordinating nucleophilic anions could provide an enthalpic driving force for the insertion of appropriate magnesium salts within the pores. A similar approach was taken previously for lithium electrolytes.¹⁰ This may result in a material with electrolyte concentrations greater than what is achievable in the bulk solutions. Further, the open metal sites may also inhibit the migration of nucleophilic anions, potentially favouring cation mobility. We therefore chose to investigate $\text{Mg}_2(\text{dobdc})$, **1**, ($\text{dobdc}^{4-} = 2,5\text{-dioxidobenzene-1,4-dicarboxylate}$),¹⁷ and its expanded analogue $\text{Mg}_2(\text{dobpdc})$, **2**, ($\text{dobpdc}^{4-} = 4,4'\text{-dioxidobiphenyl-3,3'-dicarboxylate}$).¹⁸ As depicted in Fig. 1, frameworks **1** and **2** have an identical inorganic building unit consisting of one-dimensional chains of coordinatively-unsaturated Mg^{2+} cations linked *via* oxido and carboxylato bridging moieties. In this particular series of isorecticular frameworks the pore size can be increased systematically.¹⁹

The two frameworks were soaked at 80 °C for one week in solutions consisting of a magnesium salt, either a magnesium phenolate or magnesium bis(trifluoromethanesulfonyl)imide ($\text{Mg}(\text{TFSI})_2$), dissolved in triglyme.† Note that some magnesium phenolates have recently been proposed as a component in non-pyrophoric electrolytes for magnesium batteries.²⁰ The resulting

solids were washed with triglyme to remove excess electrolyte solution from the crystallite surfaces. The materials were then filtered to yield free-flowing microcrystalline powders. Although previous electrolytes tested in magnesium batteries have typically been based on THF, triglyme offered a greater solubility of the magnesium phenolate salts, together with lower volatility.^{21–23} The use of such oligoether solvents has been previously reported in pioneering work on prototype magnesium batteries, as well as in MOF-based lithium electrolytes.^{5,24}

Inclusion of a magnesium phenolate salt within the MOF pores is expected to compete with the reversible formation of multinuclear magnesium phenolate complexes in the bulk solution that could potentially be too large to enter the framework structure.²⁵ As such, magnesium salts with less electron-donating phenolates, and thus larger dissociation constants, were anticipated to yield materials with higher magnesium phenolate loadings and thus an electrolyte loading shifted towards the framework-magnesium salt host-guest complex. The magnesium phenolates $\text{Mg}(\text{OPhMe})_2$ and $\text{Mg}(\text{OPh})_2$ exhibited a preference for the bulk solution phase, whereas $\text{Mg}(\text{OPhCF}_3)_2$, featuring a less coordinating anion, exhibited much higher concentration within the framework. It is possible that the more strongly coordinating phenolates are diffusion limited over the time scale of the experiment; no change in concentration was observed with shorter reaction times. As summarized in Table 1, the observed concentration ratios and salt loading capacities reflect the strength of the interaction between the Mg^{2+} ions and the counteranion.

The salt $\text{Mg}(\text{TFSI})_2$, which is not expected to form aggregates in solution since the TFSI^- anion is a very poor nucleophile, is also not expected to coordinate to the open metal sites lining the MOF pores. Therefore, the enthalpy gradient that drives electrolyte insertion is much smaller for $\text{Mg}(\text{TFSI})_2$ than for the magnesium phenolates, and indeed the observed loading was

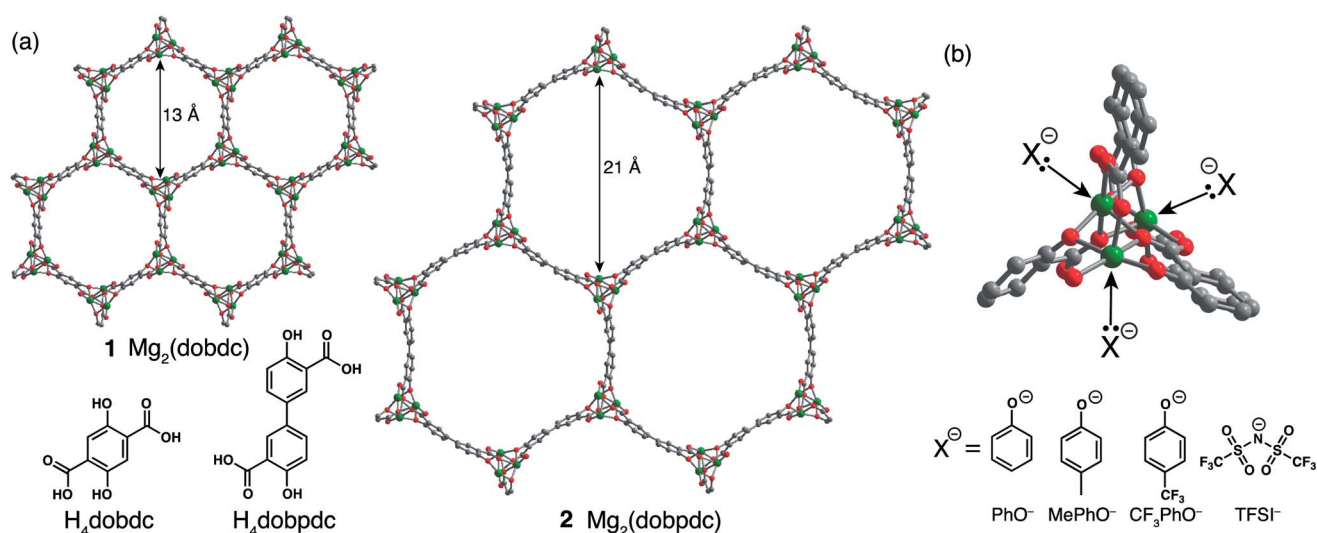
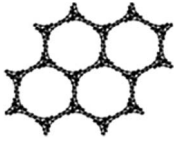
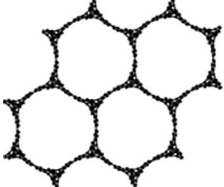


Fig. 1 (a) Structures of the metal–organic frameworks $\text{Mg}_2(\text{dobdc})$ (**1**) and $\text{Mg}_2(\text{dobpdc})$ (**2**), as viewed along the *c*-axis. The vertices of the one-dimensional channels are formed by 1-D chains of Mg^{2+} ions linked together by the respective ligands (bottom left) that form the pore walls (b) a close-up of the open coordination sites at the vertices of the pore that interact with nucleophilic guest species: PhO^- = phenolate, MePhO^- = 4-methylphenolate, CF_3PhO^- = 4-trifluoromethylphenolate, and TFSI^- = bis(trifluoromethanesulfonyl)imide.

Table 1 Summary of materials synthesized, conductivities and activation energies. Electrolyte concentrations were approximated from the unit cell volume. Concentration ratios were determined from the electrolyte concentration per unit cell as determined by elemental analysis and ^1H -NMR and the concentration of the solution that the framework was in contact with

Framework	Guest salt(s) per mole of framework	Equivalents triglyme	Electrolyte concentration (M)	$\frac{[\text{Framework}]}{[\text{Solution}]}$	Conductivity $\log_{10} (\text{S cm}^{-1})$	Molar conductivity $\log_{10} (\text{S M}^{-1} \text{cm}^{-1})$
 $\text{Mg}_2(\text{dobdc})$	$0.05\text{Mg}(\text{OPhMe})_2$	1.5	0.19	0.63	−8.1	−7.4
	$0.07\text{Mg}(\text{OPh})_2$	1.5	0.26	0.86	−7.0	−6.4
	$0.39\text{Mg}(\text{OPhCF}_3)_2$	6.0	1.5	5.0	−5.8	−6.0
	$0.06\text{Mg}(\text{TFSI})_2$	1.4	0.22	0.73	−5.8	−5.2
	$0.31\text{Mg}(\text{OPhCF}_3)_2$ and $0.30\text{Mg}(\text{TFSI})_2$	2.4	2.3	2.6 ($\text{Mg}(\text{TFSI})_2$)	−4.0	−4.4
 $\text{Mg}_2(\text{dobpdc})$	$0.31\text{Mg}(\text{OPhCF}_3)_2$	3.8	0.63	2.1	−6.2	−6.0
	$0.22\text{Mg}(\text{TFSI})_2$	3.3	0.45	1.0	−3.9	−3.6
	$0.21\text{Mg}(\text{OPhCF}_3)_2$ and $0.46\text{Mg}(\text{TFSI})_2$	4.8	1.37	2.4 ($\text{Mg}(\text{TFSI})_2$)	−3.6	−3.7

less than for $\text{Mg}(\text{OPhCF}_3)_2$. Here, the host-guest equilibrium does not favour inclusion within the MOF, since entropic factors are more significant in determining the equilibrium.

Ionic conductivities of the salt-included MOFs were measured using AC impedance spectroscopy. Samples were pressed into pellets and sandwiched between two stainless steel electrodes in a temperature-controlled cell. The frequency responses of the materials at room temperature are presented in the Nyquist and Bode plots shown in Fig. 2. The Nyquist plots all display a single semicircle at high frequency, indicating ionic conductivity through the bulk material, followed by a positively sloping capacitive tail at lower frequencies.²⁶ For more conductive samples, a significant fraction of the semicircular region is shifted beyond the high frequency limit of the instrument. The bulk conductivity for each sample was determined from the right hand minimum of the semicircle, which represents the total contribution to the impedance from ion transport through the crystal structure, grain boundaries, and interparticle interfaces.

Depending on the nature of the guest salt, ionic conductivities in **1** vary over four orders of magnitude, as reflected in the Bode plots in Fig. 2 and the conductivity values listed in Table 1. Materials containing only phenolate derivatives exhibit trends in conductivity consistent with electrolyte concentration and the expected proclivity of the guest salt for ion pairing. Thus, conductivity increases with decreasing electron-donating character of the anion. The contrast in loading and conductivity between $\text{Mg}(\text{OPhMe})_2 \subset \mathbf{1}$ and $\text{Mg}(\text{OPhCF}_3)_2 \subset \mathbf{1}$, underscores the importance that the donor ability of the anion has on the interaction with the framework, given their similarity in steric bulk. Interestingly, the conductivities of $\text{Mg}(\text{OPhCF}_3)_2 \subset \mathbf{1}$ and

$\text{Mg}(\text{TFSI})_2 \subset \mathbf{1}$ are very similar, even though the electrolyte content differs dramatically. Triglyme absorbed into $\text{Mg}_2(\text{dobdc})$ has a conductivity of 10 nS/cm, significantly smaller than the electrolyte loaded samples except in the case of $\text{Mg}(\text{OPhMe})_2$ that demonstrated exceptionally low loading. This residual ionic conductivity was attributed to charge balancing defect sites within the framework that were observed by ^1H -NMR, as discussed in the ESI.[†]

The expanded structure of **2** has a pore diameter of 21 Å and a unit cell volume of 7279 Å³, nearly double the values of 13 Å and 4005 Å³ observed for **1**. While the one-dimensional Mg^{2+} chains at the vertices of the hexagonal channels are the same, the larger organic linker decreases the polarity of the framework surface.¹⁹ This of course alters the propensity of the material for incorporating magnesium salts. In line with the increase in pore volume, the number of mole equivalents of $\text{Mg}(\text{TFSI})_2$ included more than triples, the concentration, as determined from the unit cell volume, doubles, and the calculated equilibrium constant is consistent with what would be expected for a weakly interacting guest salt (see Table 1). Remarkably, the observed ionic conductivity upon pore expansion approaches 0.1 mS cm^{−1}, representing a more than 100-fold enhancement in ionic conductivity with respect to $\text{Mg}(\text{TFSI})_2 \subset \mathbf{1}$.

The host-guest interaction is weaker in $\text{Mg}(\text{OPhCF}_3)_2 \subset \mathbf{2}$ than in $\text{Mg}(\text{OPhCF}_3)_2 \subset \mathbf{1}$, as evidenced by the decrease in the amount of $\text{Mg}(\text{OPhCF}_3)_2$ taken up from 0.39 to 0.31 equivalents under identical conditions. In a less polarizing pore environment, ion pairing is expected to be more favoured, and, accordingly, the ionic conductivity of $\text{Mg}(\text{OPhCF}_3)_2 \subset \mathbf{2}$ is less than that observed in **1**, while the molar conductivities remain similar. As such, although the host-guest interaction dominates

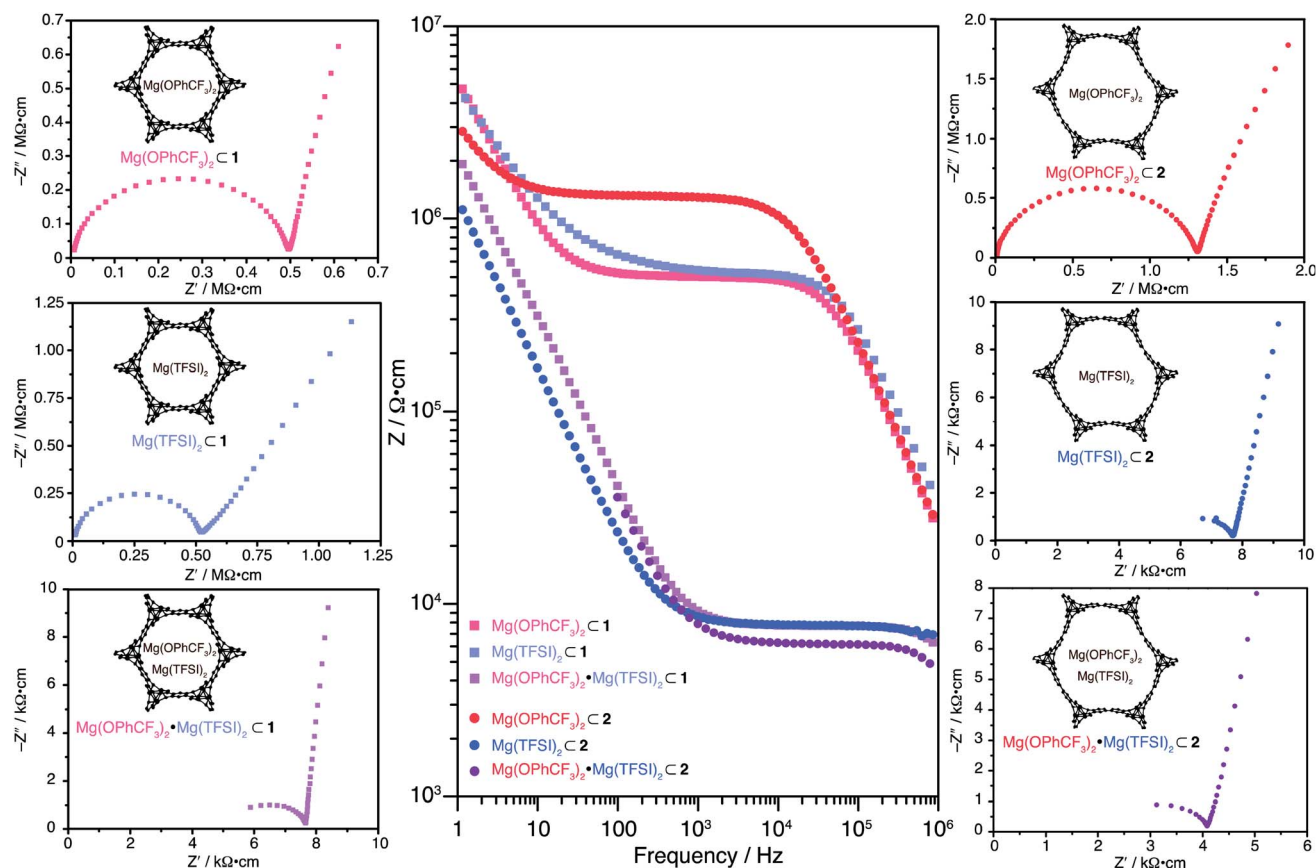


Fig. 2 AC impedance data (1 MHz to 1 Hz) at 298 K. Center: Bode plot illustrating the bulk impedance as a plateau for $\text{Mg}(\text{OPhCF}_3)_2 < 1$ (light red), $\text{Mg}(\text{TFSI})_2 < 1$ (light blue), $\text{Mg}(\text{OPhCF}_3)_2 \cdot \text{Mg}(\text{TFSI})_2 < 1$ (light purple), $\text{Mg}(\text{OPhCF}_3)_2 < 2$ (dark red), $\text{Mg}(\text{TFSI})_2 < 1$ (dark blue), and $\text{Mg}(\text{OPhCF}_3)_2 \cdot \text{Mg}(\text{TFSI})_2 < 1$ (dark purple). Left: Nyquist plots for the host framework 1 and right: Nyquist plots for the host framework 2; colors match those in the Bode plot. The left most point in the Nyquist plots corresponds to an AC frequency of 1 MHz.

guest salt inclusion, the ion mobility appears strongly dependent on the basicity of the counterion.

The similar conductivities of $\text{Mg}(\text{OPhCF}_3)_2 < 1$ and $\text{Mg}(\text{TFSI})_2 < 1$, despite the different nature and loading of the included salt, suggested to us that the interactions within the framework and transport processes for these guest electrolytes might be different enough to demonstrate a synergistic conductivity enhancement. While the nucleophilic electrolyte is strongly interacting with a single crystallite, ion transport between crystallites may be low. In contrast, the non-nucleophilic TFSI^- anion shows little or no preference for absorption in the framework. Upon soaking $\text{Mg}(\text{OPhCF}_3)_2 < 1$ overnight in a solution of $\text{Mg}(\text{TFSI})_2$, the inclusion of $\text{Mg}(\text{TFSI})_2$ increased dramatically from 0.06 to 0.3 equivalents per formula unit. More importantly, the ionic conductivity increased by two orders of magnitude with respect to either of the component guest salts alone. The expanded analogue, $\text{Mg}(\text{OPhCF}_3)_2 \cdot \text{Mg}(\text{TFSI})_2 < 2$, also showed an increase in conductivity with respect to inclusion of only one of the salts, although in this case the increase was smaller, 0.1 mS cm^{-1} to 0.25 mS cm^{-1} . These conductivity enhancements are likely explained by the relative increase in $\text{Mg}(\text{TFSI})_2$ content in the mixed salt systems, rather than the two counterions together somehow offering a significant contribution to the total conductivity. The smaller increase in conductivity of $\text{Mg}(\text{TFSI})_2$

< 2 may be attributable to this material already having a relatively high ionic conductivity, and the only modest change in $\text{Mg}(\text{TFSI})_2$ loading in the mixed salt phase. Importantly, the frameworks of 1 and 2 with dual guest salts show room-temperature ionic conductivities approaching or greater than 0.1 mS cm^{-1} , which is already 100 times greater than that reported for any other crystalline material and greater than any other solid Mg^{2+} electrolyte.^{12–16} To the best of our knowledge, this is the only class of rigid materials with ionic conductivities high enough for practical consideration as an electrolyte material in magnesium-based electrochemical cells.²⁷

Activation energies were determined by fitting variable-temperature conductivity data to the Nernst–Einstein relation (ESI^\dagger).²⁸ The resulting values varied from 0.11 eV to 0.19 eV, which is within the range of other fast ion conductors and MOF electrolytes.^{10,11,28} Ionic conductivity was found to have little dependence on the amount of solvent included in the pellet. This was evidenced by the conductivity typically increasing by less than 10–15% after saturating pressed pellets with excess triglyme, which presumably decreases contact impedance throughout the pellet. Interestingly, the materials reported here with conductivities on the order of 0.1 mS cm^{-1} maybe compared to polymer gels with similar solvent content. These MOF electrolytes are approximately 45–55 wt% solvent, as

shown in Fig. S3 and S4† by thermogravimetric analysis. Polymer gel electrolytes with comparable solvent content have demonstrated similar conductivities for $\text{Mg}(\text{TFSI})_2$.²⁹ This is in spite of the fact that the pores in polymer gels are typically one or two orders of magnitude larger than the nanometer-scale pores of the MOF electrolytes discussed here, attesting to the advantages of using a well-defined and ordered pore structure for charge transport. MOFs may also double as mechanically robust separators, and given the radically different methods by which MOFs are synthesized, new methods of cell construction and design may also be of technological interest.

Conclusions

A series of MOF-based magnesium electrolytes were prepared and their ionic conductivities assessed by AC impedance spectroscopy. By increasing pore size and tuning the anion basicity of guest electrolyte salts, conductivity values were found to vary over four orders of magnitude, and reaching values as high as 0.25 mS cm^{-1} . These frameworks can be considered rigid solid-state electrolyte alternatives to state-of-the-art gel electrolyte systems and may be of particular interest for developing new methods of cell construction and design for magnesium batteries. Although here only the pore size and the structure of the guest salt were varied, particle morphology, crystallite size, solvent polarity, and framework topology, amongst other parameters, are also expected to have a significant impact on the charge transport properties MOF electrolytes. Future work will focus on evaluating the performance of the new electrolytes in full electrochemical cells—importantly, preliminary results already show these materials to be stable against solid magnesium electrodes without passivation. We also seek to further improve the ionic conductivity and develop new methods for preparing solvent-free MOF electrolytes.

Acknowledgements

This research was supported by the United States Department of Energy, Energy Efficiency and Renewable Energy, Hydrogen and Fuel Cell Program. R.A. thanks the Research Foundation Flanders (FWO – Vlaanderen) for a postdoctoral fellowship. We thank Mr David Gygi for experimental assistance and Prof. Nitash Balsara for experimental assistance and helpful discussion.

Notes and references

† Similar or lower electrolyte loadings were observed with shorter reaction times for electrolyte incorporation in $\text{Mg}_2(\text{dobdc})$. The reaction was attempted with $\text{Ni}_2(\text{dobdc})$ as well but lower electrolyte loadings were observed under identical reaction conditions.

- 1 J. R. Long and O. M. Yaghi, *Chem. Soc. Rev.*, 2009, **38**, 1213.
- 2 M. Eddaoudi, J. Kim, N. Rosi, D. Vodak, J. Wachter, M. O'Keeffe and O. M. Yaghi, *Science*, 2002, **295**, 469.
- 3 Z. Q. Wang and S. M. Cohen, *Chem. Soc. Rev.*, 2009, **38**, 1315.

- 4 F. Stallmach, S. Gröger, V. Künzel, J. Kärger, O. M. Yaghi, M. Hesse and U. Müller, *Angew. Chem., Int. Ed.*, 2006, **45**, 2123.
- 5 N. Yanai, T. Uemura, S. Horike, S. Shimomura and S. Kitagawa, *Chem. Commun.*, 2011, **47**, 1722.
- 6 A. Morozan and F. Jaouen, *Energy Environ. Sci.*, 2012, **5**, 9269.
- 7 S. Bureekaew, *Nat. Mater.*, 2009, **8**, 831.
- 8 J. Hurd, R. Vaidhyanathan, V. Thangadurai, C. I. Ratcliffe, I. L. Moudrakovski and G. K. H. Shimizu, *Nat. Chem.*, 2009, **1**, 705.
- 9 M. Yoon, K. Suh, S. Natarajan and K. Kim, *Angew. Chem., Int. Ed.*, 2013, **52**, 2688.
- 10 B. M. Wiers, M. L. Foo, N. P. Balsara and J. R. Long, *J. Am. Chem. Soc.*, 2011, **133**, 14522.
- 11 R. Ameloot, M. Aubrey, B. M. Wiers, A. P. Gómora-Figueroa, S. N. Patel, N. P. Balsara and J. R. Long, *Chem.-Eur. J.*, 2013, **19**, 5533.
- 12 M. S. Whittingham, *Solid State Ionics*, 1989, **32–33**, 344.
- 13 A. Omote, S. Yotsuhashi, Y. Zenitani and Y. Yamada, *J. Am. Ceram. Soc.*, 2011, **94**, 2285.
- 14 J. C. McKeen and M. E. Davis, *J. Phys. Chem. C*, 2009, **113**, 9870.
- 15 N. Yoshimoto, Y. Tomonaga, M. Ishikawa and M. Morita, *Electrochim. Acta*, 2001, **46**, 1195.
- 16 S. Higashi, K. Miwa, M. Aoki and K. Takechi, *Chem. Commun.*, 2013, DOI: 10.1039/c3cc47097k.
- 17 S. R. Caskey, A. G. Wong-Foy and A. J. Matzger, *J. Am. Chem. Soc.*, 2008, **130**, 10870.
- 18 T. M. McDonald, W. R. Lee, J. A. Mason, B. M. Wiers, C. S. Hong and J. R. Long, *J. Am. Chem. Soc.*, 2012, **134**, 7056.
- 19 H. X. Deng, S. Grunder, K. E. Cordova, C. Valente, H. Furukawa, M. Hmadeh, F. Gándara, A. C. Whalley, Z. Liu, S. Asahina, H. Kazumori, M. O'Keeffe, O. Terasaki, J. F. Stoddart and O. M. Yaghi, *Science*, 2012, **336**, 1018.
- 20 F. F. Wang, Y. S. Guo, J. Yang, Y. Nuli and S. Hirano, *Chem. Commun.*, 2012, **48**, 10763.
- 21 D. Aurbach, Z. Lu, A. Schechter, Y. Gofer, H. Gizbar, R. Turgeman, Y. Cohen, M. Moshkovich and E. Levi, *Nature*, 2000, **407**, 724.
- 22 J. Muldoon, C. B. Bucur, A. G. Oliver, T. Sugimoto, M. Matsui, H. S. Kim, G. D. Allred, J. Zajicek and Y. Kotani, *Energy Environ. Sci.*, 2012, **5**, 5941.
- 23 H. S. Kim, T. S. Arthur, G. D. Allred, J. Zajicek, J. G. Newman, A. E. Rodnyansky, A. G. Oliver, W. C. Boggess and J. Muldoon, *Nat. Commun.*, 2011, **2**, 427.
- 24 D. Aurbach, H. Gizbar, A. Schechter, O. Chusid, H. E. Gottlieb, Y. Gofer and I. Goldberg, *J. Electrochem. Soc.*, 2002, **149**, A115.
- 25 L. Albaric, N. Hovnanian, A. Julbe, C. Guizard, A. Alvarez-Larena and J. F. Piniella, *Polyhedron*, 1997, **16**, 587.
- 26 R. A. Huggins, *Advanced batteries: materials science aspects*, Springer Science, New York, 2008, pp. 339–373.
- 27 E. Quartarone and P. Mustarelli, *Chem. Soc. Rev.*, 2011, **40**, 2525.
- 28 R. G. Linford and S. Hackwood, *Chem. Rev.*, 1981, **81**, 327.
- 29 N. Yoshimoto, S. Yakushiji, M. Ishikawa and M. Morita, *Electrochim. Acta*, 2003, **48**, 2317.